Flow on Grooved Roof Surface

Yoon, Tae Hoon* · Hwang, Chang Ho**

ABSTRACT/Spatially varied unsteady flow in a groove-like channel of a sloping roof is analyzed by numerical solution of Saint Venant equations. Depth variations are discussed with different slopes and bed roughness of the channel. Time to equilibrium is found to be inversely proportional to the kinematic flow number. The design of roof drainage system by different schemes is included.

1. Introduction

An overland flow is governed by factors such as surface and rainfall characteristics. They may be length, slope, roughness and infiltration of the surface, and intensity and duration of the rainfall. The overland flow with rainfall as lateral inflow is varied in space and time resulting in a spatially varied unsteady flow. Morgali and Linsley(7) seem to have been one of the first to apply numerical method to the solution of the overland flow. The same approach was followed by many others(1, 2, 3, 6, 9, 11). With advantage that analytic solution is possible for simple geometries, kinematic wave solution has been paid attention from many parts such as Brakensiek(3), Constatinides(5), Overton and Meadows(8), Stephenson and Meadows(10) and Woolhiser(12).

One of the situations, from which the spatially varied unsteady flow can be observed, is a roof drainge problem. Some roof structures of large manufactuaring plant and large warehouse in general consisted of wavy panels. The wavy panels form grooves termed herein groove-like channel in which rainwater runs down. If the groove-like channel is long enough in the direction

* Prof., Dept., of Civil Eng., Hanyang Univ.

** Research Assistant, Dept., of Civil Eng., Hanyang Univ.

of the flow, the groove–like channel may be overflowed in the downstream portion during heavy rainfall, and the water overflowed penetrates into the plant or warehouse. Such a functional failure may cause a serious damage to facilities and assets. For the proper design of roof structures, the knowledge about the spatially varied unsteady flow in the groove–like channel is essential. In this study, the unsteady nonuniform flow in the groove–like channel is analyzed by numerical schemes.

2. Governing Equations

The slope of groove–like channel in a roof drainage is mild, then flow may be downstream controlled and affected by a backwater. For accurate representation of such a flow, full Saint Venant equations are necessary. The governing equations are formulated with the following assumptions : (1) flow is unidirectional and velocity in the groove is uniform ; (2) the pressure is hydrostatic ; (3) overpressure introduced by rainfall is negligible and velocity components of the rainfall in the x–direction is zero ; (4) rainfall intensity is uniform in space and time.

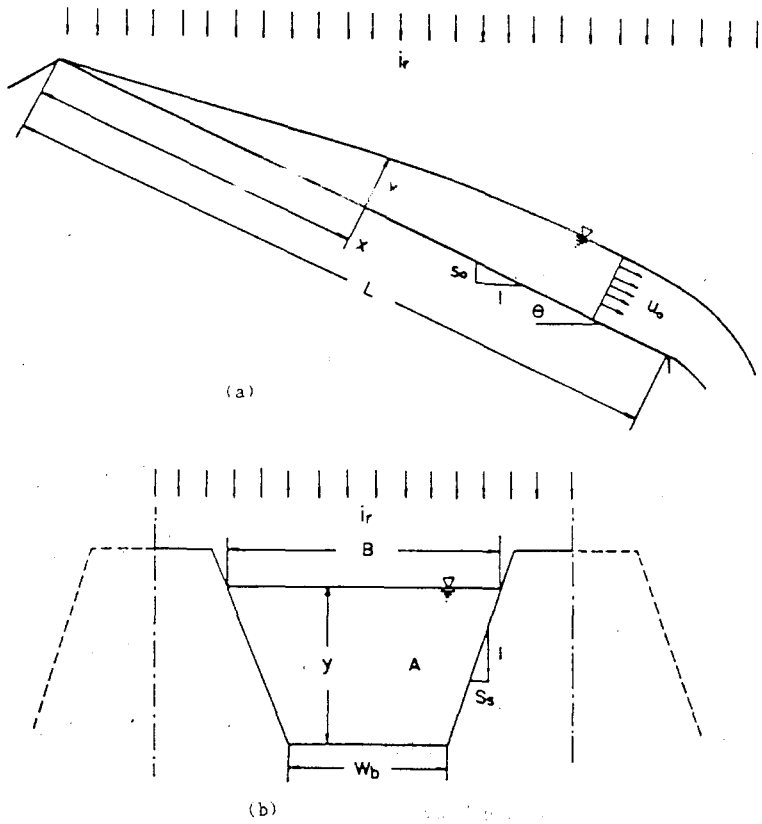

Fig. 1 Definition sketch

$$\frac{\partial A}{\partial t}+\frac{\partial Q}{\partial X}=i_r \tag{1}$$

$$\frac{\partial Q}{\partial t}+\frac{\partial}{\partial X}\left[\frac{Q^2}{A}\right]+\cos\theta\ \ gA\frac{\partial y}{\partial x}=gA(S_0-\cos\theta\ \ S_f)-ir\ \frac{Q}{A} \tag{2}$$

in which Q is discharge at x, S_f is friction slope, S_o bottom slope, A flow sectional area, i_r rainfall intersiy as a lateral inflow, θ angle between the channel bottom and the horizon, g the gravitational acceleration, x the distance along the channel, and t time.

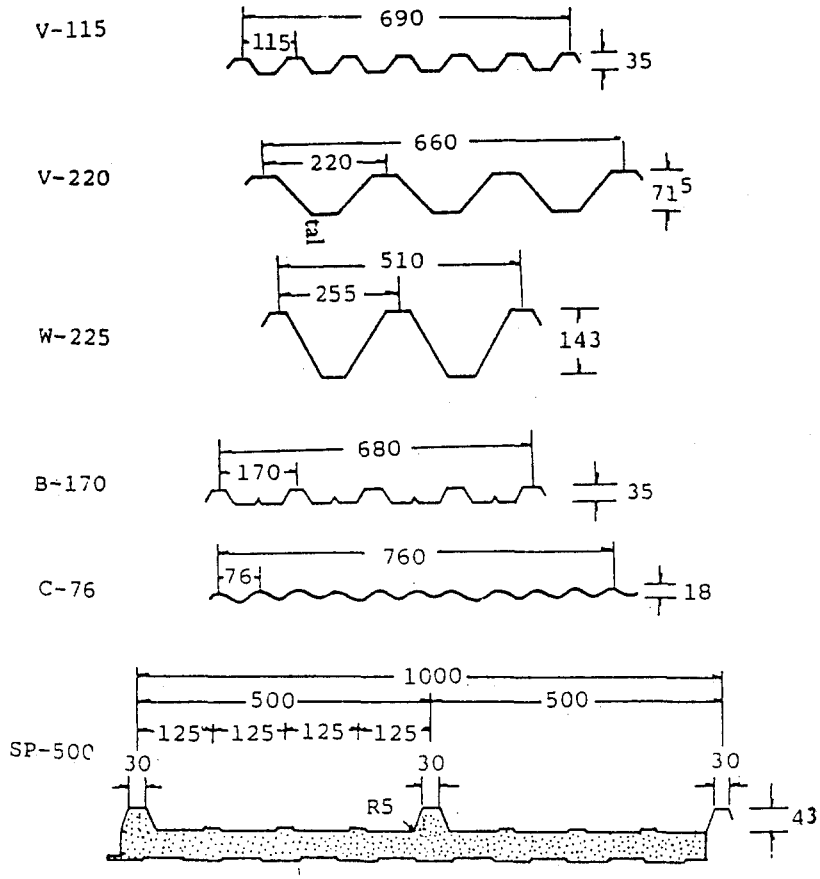

Fig. 2 Various sections of roof panel

The friction slope is given by Manning equation as

$$S_f=\frac{n^2Q\mid Q\mid}{A^2R^{4/3}} \tag{3}$$

in which R is hydraulic radius and n is Manning roughness coefficient.

For slopes greater than 0.14, the vertical distance from the channel bed to the water surface y

differs from the depth normal to the bed d by greater than 1 percent. For slopes of 0.14 or greater, the difference between the piezometric head and y is greater than 1 percent. Hence, for slopes of roof system steeper than 0.14, the effect of bed slope on the terms such as pressure and friction in the momentum equation may not be neglected. But cos θ of the term cos θ S_f is effective only for a channel cross section approximating a triangular section or similar one. Fig. 2 shows the various cross sections of roof system widely used and sp–500 in the figure was used in this study.

Derivatives of A is transformed to that of y by $dA/dy = B$. For easy manipulation the governing equations are nondimensionalized.

Nondimensional variables are defined as:

$$X = x/L,\ Yy/y_o,\ B^* = B/y_o,\ A^* = A/y_o^2,\ T = tu_o/L,\ U = u/u_o,\ I_r = i_rL/u_oy_o^2,\ Q^* = Q/u^oy_o^2$$

where y_o is the normal depth at the downstream end($x = L$), and u_o is the velocity corresponding to y_o. Using these variables the friction slope is written as

$$S_f = C_f \frac{Q\,|Q|}{A^2R^{4/3}} \tag{4}$$

in which $C_f = n^2u_o^2/y_o^{4/3}$. For the sake of simplicity, the asteriks are removed hereafter. With the variables and Eq.4, Eqs.1 and 2 yield

$$B\frac{\partial Y}{\partial T} + \frac{\partial Q}{\partial X} = Ir \tag{5}$$

$$\frac{\partial Q}{\partial T} - \frac{2QB}{A}\frac{\partial Y}{\partial T} - \left(\frac{Q^2B}{A^3} - \cos\theta\,\frac{A}{F_0^2}\right)\frac{\partial Q}{\partial X} = KA\left(1 - \frac{\cos\theta}{S_0}C_f\frac{Q\,|Q|}{A^2R^{4/3}}\right) - 3Ir\frac{Q}{A} \tag{6}$$

where k is the kinematic flow number

$$k = \frac{S_0L}{y_0F_0^2} \tag{7}$$

and F_o is the Froude number defined as

$$F_0 = \frac{u_0}{\sqrt{gy_0}}$$

3. Initial and boundary conditions

Initially the roof surface is a dry bed for which all flows and depths are zero at the time rainfall commences($t = 0$). The zero depth, however, is modified to circumvent the difficulties of division by zero, and hence nonzero initial depth is specified.

$$Y(x,0) = 0.01Y_o$$
$$Q(x,0) = 0 \tag{8}$$

No flow entered the upstream boundary, the velocity there is zero for all time. This means all flow will enter the roof groove as rainfall. Morgali and Linsley(7) and Brutsaert(4) used the continuity equation to obtain the upstream boundary depth. If the slope is mild and flow is subcritical, the depth at the upper boundary may be affected by the storage at the upper most section or by the backwater. Hence, the continuity equation may not provide proper depth at the upstream end. To avoid such a drawback in this study a symmetric condition is used as in Fig.3.

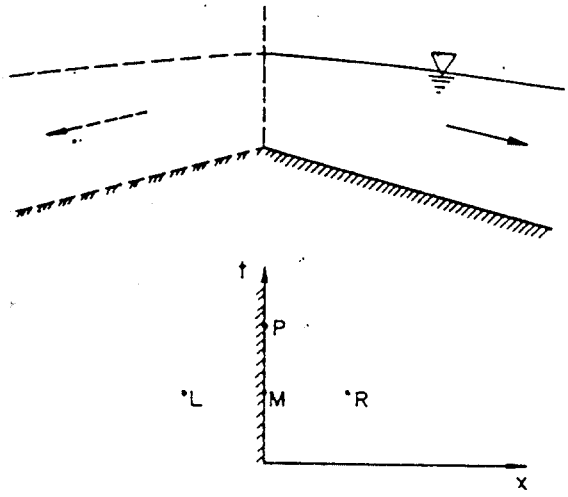

Fig. 3 Symmetric boundary

$$U(0,t) = 0$$
$$U_L = -U_R \tag{9}$$
$$Y_L = Y_R$$

At the downstream boundary a critical depth occurs if flow is subcritical. A proper downstream boundary condition is to specify a critical depth for a free overfall.

$$Y(L,t) = Y_c \tag{10}$$

If the flow is supercritical, no boundary condition is needed to specify.

4. Finite Difference Formulation.

In finite difference formulation a central difference is used for space and forward differece for time. The resulting implicit finite difference forms of Eqs.5 and 6 are written as

$$\frac{D_1}{\Delta T}(Y_i^{j+1}-Y_i^j)+\frac{1}{2\Delta X}\left[\frac{1}{2}(Q_{i+1}^{j+1}+Q_{i+1}^j)-\frac{1}{2}(Q_{i-1}^{j+1}+Q_{i-1}^j)\right]=I_r \tag{11}$$

$$\frac{Q_i^{j+1}-Q_i^j}{T}-D_2\frac{Y_i^{j+1}-Y_i^j}{\Delta T}-D_3\frac{\frac{1}{2}(Y_{i+1}^{j+1}+Y_{i+1}^j)-\frac{1}{2}(Y_{i-1}^{j+1}+Y_{i-1}^j)}{2X}$$

$$=D_4(1-D_5\mid Q_i^j\mid Q_i^{j+1})-D_6 \tag{12}$$

in which

$$D_1=B,\quad D_2=\frac{2QB}{A},\quad D_3=\frac{Q^2B}{A^2}-\cos\theta\frac{A}{F_0^2}$$

$$D_4=KA,\quad D_5=\frac{\cos\theta}{S_0}C_f\frac{1}{A^2R^{3/3}},\quad D_6=\frac{3IrQ}{A} \tag{13}$$

Eq.12 is nonlinear equation. In order to avoid difficulties in nonlinearity D_1 through D_6 computed at time step $T = j\Delta T$ are used in the computation at time step $T = (j + 1)\Delta T$, which makes Eq.12 linear.

5. Result Analysis

The computations are carried out for different conditions such as varying channel slopes and varying channel roughness, which ranges n = 0.012 for steel to n = 0.016 for rough concrete. Lateral inflow was kept as single uniform rainfall intensity. In this study the rainfall intensity of

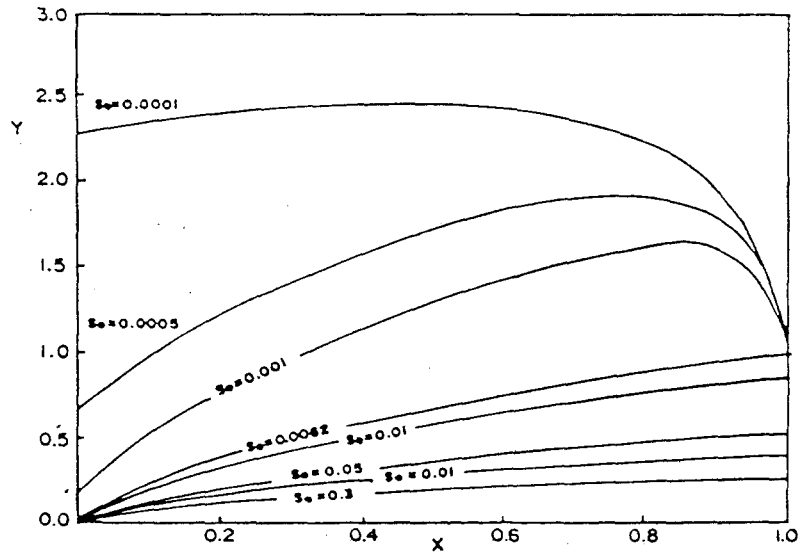

Fig. 4 Depth variation with slopes(n = 0.012)

120 mm/hr is used.

Fig. 4 through 6 show the variations of depth with slopes for different roughness. From the figures some significant facts are noted: for all cases the same critical depth is found since the rainfall is kept constant resulting in the same discharge; for each given roughness a critical slope is obtained ; very common fact which depth increases with decreasing slope and increasing roughness.

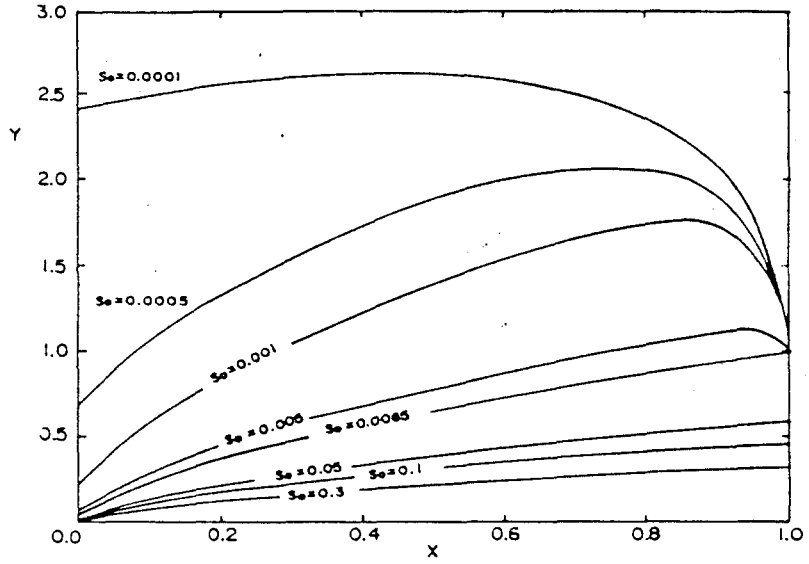

Fig. 5 Depth variation with slopes(n = 0.014)

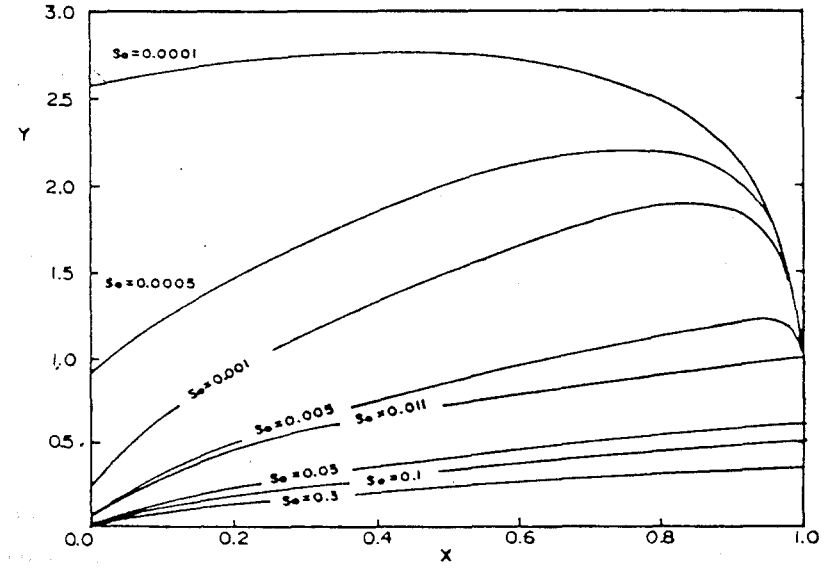

Fig. 6 Depth variation with slopes(n = 0.016)

F_o	S_o	n	k
1	0.0062	0.012	42
1	0.0085	0.014	57
1	0.0110	0.016	75

The roughness values, kinematic flow number k and slopes S_o for critical flow are summarized above. Considering that kinematic wave method is applicable to rather rapid flow, criterion for applying the kinematic wave method may change with slope and roughness. Fig. 7 shows the relation between the time to equilibrium, t_e in second to kinematic flow number k. As can be expected t_e is attained earlier with large k since large k goes wih rapid flow. This, however, is a special case since it does not include lateral inflow or rainfall intensity, and differs from the result of Morgali and Linsley(7).

$$t_c=59.6\frac{L^{0.593}n^{0.605}}{q^{0.388}S_o^{0.38}} \tag{14}$$

in which q is rainfall intensity in inches per hour. Similar result was obtained by Woolhiser and Liggett(11).

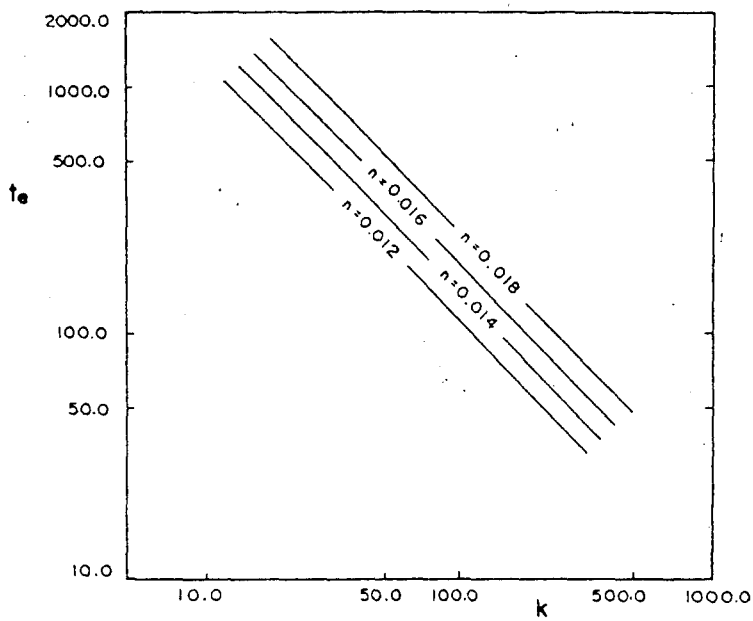

Fig. 7 Time to Equilibrium

Max. depth occurs at the downstream end or brink for supercritical flow. For subcritical flow, however, the depth at the brink is close to critical depth and max. depth occurs upstream from the brink and moves upstream as flow is slowing down as shown in Fig.8.

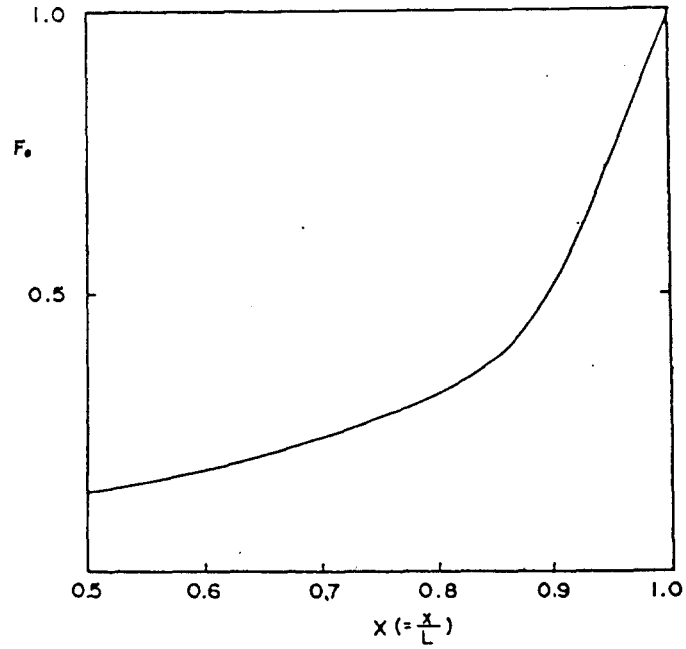

Fig. 8 Location of maximum depth

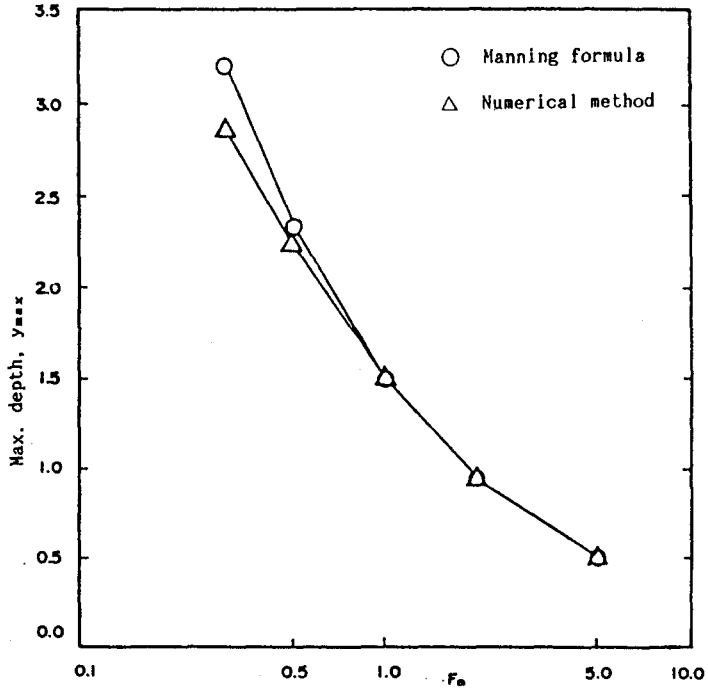

Fig. 9 Maximum depth by Manning formula and numerical method

In the design of roof drainage system, general practice has been using Manning formula. It is worthwhile to compare the max. depths computed by numerical method and Manning formula as shown in Fig.9. No difference is expected in supercritical flow. In subcritical flow, however, numerical method has smaller depth than Manning formula. It may be ascribed to the movement of the max. depth upstream and consquently it has less rainfall up to the point of max. depth resulting in less discharge. Form Fig.9 it is noted that design by Manning formula is at safe side.

To see how significant the term of $\cos\theta$ in the momentum equation is on depth, max. depths with and without $\cos\theta$ are calculated and shown in Fig.10. For slopes greater than 50% or higher the difference is sizable.

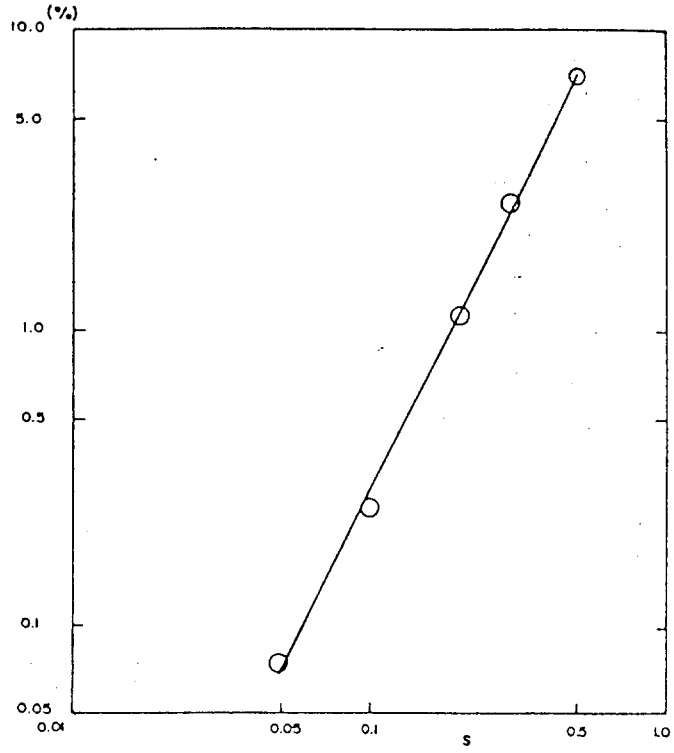

Fig. 10 Depth difference with and without $\cos\theta$ term in momentum equation

5. Conclusions

Flow of the roof drain, which is spatially varied unsteady flow and described by Saint Venant equation, is analyzed by numerical scheme. In a groove–like channel, channel bed roughness and channel slope are found to be much more dominant factors on depth variation. Time to equilibrium is found to be inversely propotinal to the kinematic flow number. In subcritical flow, the max. depth computed by numerical method is less than that by Manning formula and the

latter is at safe side in design of roof drain. In steep roof drainage system, the effect of bed slope appeared as $\cos\theta$ in the momentum equation is also found not to be negligible. For the complete analysis, further work is needed for different rainfall intensity.

References

1. Brankensiek, D. L. (1966) Hydrodynamics of overland flow and nonprismatic channel, Trans. ASCE, pp.119–122.
2. Brankensiek, D. L., A. L. Heath and G. H. Comer, (1966) Numerical technique for small watershed flood routing, U. S. Dept. of Agriculture, ARS, Feb., pp.41–113.
3. Brankensiek, D. L. (1967) Kinematic flood routing, ASCE, Trans. Vol.10, part 3, pp.340–343.
4. Brutsaert, W. (1971) De Saint–Venant equations experimentally verified, J. of Hydraulic Div., ASCE, Vol. 97, No. HY9, Sept. pp.1387–1400.
5. Constantinides, C. A. (1981) Numerical technique for two–dimensional kinematic overland flow model, Water SA, 7(4), pp,234–248.
6. Liggett, J. A. and D. A. (1967) Woolhiser, Difference solution of the shallow water equation, J. of Eng. Mech. Div., ASCE, Vol.93, No. EM2, April, pp.39–71.
7. Morgali, J. R. and R. K. Linsley, (1965) Computer analysis of overland flow, J. of Hyd. Div., ASCE, Vol. 91, No. HY3, May. pp.81–100.
8. Overton, D. E. and M. E. (1976) Meadows, Stormwater modelling, Academic Press, New York.
9. Schaake, J. C. (1965) Synthesis of the inlet hydrograph, Technical Report No. 3, Storm Drainage Research Proj., Dept. of San. Eng. and Water Resources, The Johns Hopkins Univ., Boltimore, Md. June.
10. Stephenson, D. and M. E. Meadows, (1986) Kinematic hydrology and modelling, Developments in water science, No. 26, Elsevier science publisher, Amsderdam.
11. Woolhiser, D. A. and J. A. Liggett, (1967) Unsteady one–dimensional flow over a plan–the risign hydrograph, water Resources Research, Vol. 3, No. 3.
12. Woohiser, D. A. (1975) Simulation of unsteady overland flow, Unsteady flow in open channel, ed. K. Mahmood and V. Yevjevich, Vol. , Water Resources Publications, Colorado.